Hindawi
Advances in Mathematical Physics
Volume 2019, Article ID 7203408, 8 pages
https://doi.org/10.1155/2019/7203408

Research Article

Application of the Complex Variable Function Method to SH-Wave Scattering Around a Circular Nanoinclusion

Hongmei Wu [1,2]

[1] *School of Mechanical and Electronical Engineering, Lanzhou University of Technology, Lanzhou, Gansu, China*
[2] *School of Science, Lanzhou University of Technology, Lanzhou, Gansu, China*

Correspondence should be addressed to Hongmei Wu; wuhongmei0610@126.com

Received 13 December 2018; Revised 30 January 2019; Accepted 20 February 2019; Published 20 March 2019

Academic Editor: Zengtao Chen

This paper focuses on analyzing SH-wave scattering around a circular nanoinclusion using the complex variable function method. The surface elasticity theory is employed in the analysis to account for the interface effect at the nanoscale. Considering the interface effect, the boundary condition is given, and the infinite algebraic equations are established to solve the unknown coefficients of the scattered and refracted wave solutions. The analytic solutions of the stress field are obtained by using the orthogonality of trigonometric function. Finally, the dynamic stress concentration factor and the radial stress of a circular nanoinclusion are analyzed with some numerical results. The numerical results show that the interface effect weakens the dynamic stress concentration but enhances the radial stress around the nanoinclusion; further, we prove that the analytic solutions are correct.

1. Introduction

Because of scattering's important role in understanding various wave propagation phenomena in engineering materials and structures, elastic waves' scattering by a cavity/inclusion embedded in an elastic matrix currently is a popular topic in wave motion. Through the methods of wave functions expansion, integral equations, and integral transform, Mow and Pao [1] discussed in detail a cavity/inclusion in an elastic medium' diffraction of elastic waves. Liu [2] studied dynamic stress concentration around a circular hole attributable to SH-wave in anisotropic media using the method of complex variable function. Subsequently, Liu et al. [3] studied SH-waves' scattering and dynamic stress concentration by interface cylindrical elastic inclusion. Recently, Hei [4] modelled and analyzed the dynamic behavior of an inhomogeneous continuum containing a circular inclusion, while Mcarthur et al. [5] discussed a circular inclusion with circumferentially inhomogeneous imperfect interface in harmonic materials. Further, Jiang [6] studied a shallow circular inclusion's dynamic response under incident SH-waves in a radially inhomogeneous half-space and analyzed it applying complex function theory and the multipolar coordinate system.

However, the research mentioned above was carried out at the macroscale, and, thus, the surface/interface stress effect was not taken into account. However, because of the rapid development of nanoscience and nanotechnology, it is essential to know nanomaterials and structures' mechanical behavior. At the nanoscale, the surface/interface effect becomes significant because of the increasing ratio of the surface to bulk volume [7]. Gurtin et al. [8] presented the theory of surface elasticity that considers the surface or interface elasticity, and Miller and Shenoy's [9, 10] results agreed well with direct atomic simulations. Therefore, the surface elasticity theory has been applied widely to study various mechanical behaviors at the nanoscale [11, 12]. Using Gurtin's surface elasticity theory, Wang et al. [13, 14] considered nanocavities' diffraction by the P-wave, while Wang [15] analyzed the surface effect of two circular cylindrical holes' multiple diffractions of the P-wave. Further, Ou [16] discussed interface energy's effects on plane elastic waves's scattering by a nanosized coated fiber. Ru et al. [17–19] investigated elastic waves' diffraction around a cylindrical nanoinclusion and then studied the surface effect of vertical shear wave's scattering by a cluster of nanosized cylindrical holes. Further, Wu [20] investigated the interface effect of SH-waves' scattering by a cylindrical nanoinclusion. However,

most of these studies used the wave function expansion method to discuss such problems, while very few have used the complex variable function method to solve them. Therefore, it is imperative to investigate such problems by the complex variable function method.

In this work, SH-waves' scattering around a circular nanoinclusion is studied within the framework of surface elasticity, in which the analytical solutions of displacement fields are expressed by employing the method of complex variable function, and the numerical results of dynamic stress concentration factor and the radial stress of a circular nanoinclusion are illustrated graphically. The paper is organized as follows. A brief introduction to the theory of surface elasticity is presented in Section 2. Section 3 describes the way the complex variable function is adopted to derive the solutions for the elastic fields that incident SH-wave induces around a circular nanoinclusion and presents the governing equations and boundary conditions for the problem. In Section 4, the dynamic stress concentration factor and the radial stress of a circular nanoinclusion are analyzed and the numerical results are presented. Our concluding remarks are presented in Section 5.

2. Basic Equations of Surface Elasticity

According to the surface elasticity theory, a surface is considered to be a negligible film that adheres to the matrix without slipping. Classical elastic theory still applies to the matrix, but the presence of surface stress leads to nonclassical boundary conditions. The equilibrium equations and the isotropic constitutive relations in the matrix are the same as those in the classical elasticity theory:

$$\sigma_{ij,j} = \rho \frac{\partial^2 u_i}{\partial t^2} \tag{1}$$

$$\sigma_{ij} = 2\mu\left(\varepsilon_{ij} + \frac{\nu}{1-\nu}\varepsilon_{kk}\delta_{ij}\right) \tag{2}$$

in which t is time, ρ is the material's mass density, μ and ν are the shear modulus and Poisson's ratio, respectively, and σ_{ij} and ε_{ij} are stress and strain tensors in the bulk material, respectively. The strain tensor is related to the displacement vector u_i by

$$\varepsilon_{ij} = \frac{1}{2}\left(u_{i,j} + u_{j,i}\right) \tag{3}$$

The surface stress tensor $\sigma^s_{\alpha\beta}$ is related to the surface energy density G by

$$\sigma^s_{\alpha\beta} = \tau^0\delta_{\alpha\beta} + \frac{\partial G}{\partial \varepsilon_{\alpha\beta}} \tag{4}$$

in which $\varepsilon_{\alpha\beta}$ is the second-rank tensor of surface strain, $\delta_{\alpha\beta}$ is the Kronecker delta, and τ^0 is the residual surface tension under unstrained condition. Einstein's summation convention is adopted for all repeated Latin indices $(1, 2, 3)$ and Greek indices $(1, 2)$ throughout the paper.

Assume that the interface adheres perfectly to the matrix material without slipping. By the generalized Young-Laplace equation, the equilibrium equations and the constitutive relations on the surface are

$$\left(\sigma - \sigma^I\right)\boldsymbol{n} = -\nabla_s \cdot \sigma^s \tag{5}$$

$$\begin{aligned}\sigma^s_{\alpha\beta} = {} & \tau^0\delta_{\alpha\beta} + 2\left(\mu^s - \tau^0\right)\delta_{\alpha\gamma}\varepsilon_{\gamma\beta} \\ & + \left(\lambda^s + \tau^0\right)\varepsilon_{\gamma\gamma}\delta_{\alpha\beta}\end{aligned} \tag{6}$$

in which σ, σ^I, σ^s are matrix, inclusion, and interface stress, respectively, and $\nabla_s \cdot \sigma^s$ is the interface divergence. $\boldsymbol{n}$ denotes the normal vector of the surface, and μ^s and λ^s are two surface constants.

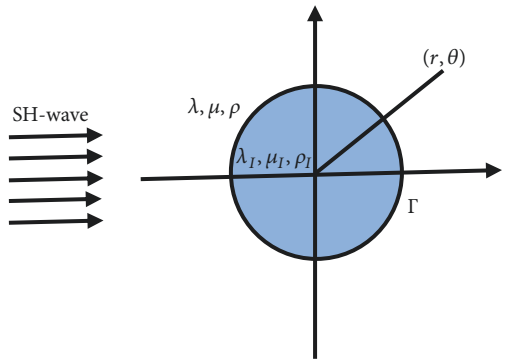

Figure 1: The scattering of SH-wave around a circular nanoinclusion.

3. Scattering of SH-Wave around a Circular Nanoinclusion

Based on the surface elasticity theory, we discuss the scattering of SH-wave around a circular nanoinclusion embedded in an infinite elastic medium, in which λ, μ, ρ, and λ_I, μ_I, ρ_I are the matrix and inclusion's parameters, respectively, and Γ is the interface between the inclusion and the matrix, as illustrated in Figure 1.

For the antiplane problem, we have

$$\begin{aligned} u_x &= u_y = 0, \\ u_z &= w(x, y)\end{aligned} \tag{7}$$

The antiplane governing equation in the matrix is

$$\frac{\partial \sigma_{xz}}{\partial x} + \frac{\partial \sigma_{yz}}{\partial y} = \rho\frac{\partial^2 w}{\partial t^2} \tag{8}$$

in which σ_{xz}, σ_{yz} are the shear stresses in the bulk.

The relation between stress and displacement is

$$\begin{aligned} \sigma_{xz} &= \mu\frac{\partial w}{\partial x}, \\ \sigma_{yz} &= \mu\frac{\partial w}{\partial y}\end{aligned} \tag{9}$$

Substituting (9) into (8), we obtain the following equation:

$$\frac{\partial^2 w}{\partial x^2} + \frac{\partial^2 w}{\partial y^2} = \frac{\rho}{\mu}\frac{\partial^2 w}{\partial t^2} \tag{10}$$

For the steady-state response, the dependence on time may be separated as $w = We^{-i\omega t}$, and then (10) can be written as follows:

$$\nabla^2 W + K^2 W = 0 \tag{11}$$

in which W is the displacement function, $K = \omega/v$ is the wave number, $v = \sqrt{\mu/\rho}$ is the media's shear velocity, ω is the circular frequency, and μ and ρ are the matrix' shear modulus and mass density, respectively.

Based on the complex variable function theory, we introduce complex variables $z = x + iy$, $\overline{z} = x - iy$. Equations (11) and (9) are

$$\frac{\partial^2 W}{\partial z \partial \overline{z}} + \frac{1}{4}K^2 W = 0 \tag{12}$$

$$\begin{aligned} \sigma_{xz} &= \mu\left(\frac{\partial W}{\partial z} + \frac{\partial W}{\partial \overline{z}}\right), \\ \sigma_{yz} &= i\mu\left(\frac{\partial W}{\partial z} - \frac{\partial W}{\partial \overline{z}}\right) \end{aligned} \tag{13}$$

In the cylindrical coordinate system (r, θ, z), (13) can be expressed as

$$\begin{aligned} \sigma_{rz} &= \mu\left(\frac{\partial W}{\partial z}e^{i\theta} + \frac{\partial W}{\partial \overline{z}}e^{-i\theta}\right), \\ \sigma_{\theta z} &= i\mu\left(\frac{\partial W}{\partial z}e^{i\theta} - \frac{\partial W}{\partial \overline{z}}e^{-i\theta}\right) \end{aligned} \tag{14}$$

Assume that a harmonically plane SH-wave propagates in the positive x-direction, as shown in Figure 1. According to (12), the general solution of incident SH-wave function $W^{(Inc)}$ is expressed as [1]:

$$W^{(Inc)} = W_0 e^{iKx} = W_0 e^{(iK/2)(z+\overline{z})} \tag{15}$$

The scattered wave function $W^{(Sca)}$ in the curvilinear coordinates is expressed as [1]:

$$W^{(Sca)} = \frac{1}{2}W_0 \sum_{n=0}^{+\infty} A_n H_n^{(1)}\left[K|z|\right]\left[\left(\frac{z}{|z|}\right)^n + \left(\frac{z}{|z|}\right)^{-n}\right] \tag{16}$$

in which W_0 is the incident wave's amplitude, $H_n^{(1)}(\cdot)$ is the nth order Hankel function of the first kind, and A_n are unknown coefficients the boundary conditions determined.

The displacement potential of the refracted wave in the inclusion can be expressed as [1]:

$$W^{(Ref)} = -\frac{1}{2}W_0 \sum_{n=0}^{+\infty} B_n J_n\left[K_I|z|\right]\left[\left(\frac{z}{|z|}\right)^n + \left(\frac{z}{|z|}\right)^{-n}\right] \tag{17}$$

in which $J_n(\cdot)$ is the nth order Bessel function of the first kind, B_n are unknown coefficients the boundary conditions determined, $K_I = \omega/v_I$ is the wave number of the inclusion, $v_I = \sqrt{\mu_I/\rho_I}$ is the inclusion's shear velocity, and μ_I and ρ_I are the inclusion' shear modulus and mass density, respectively.

The total wave function in the elastic medium and the nanoinclusion are determined by

$$\begin{aligned} W^{(M)} &= W^{(Inc)} + W^{(Sca)}, \\ W^{(I)} &= W^{(Ref)} \end{aligned} \tag{18}$$

Substituting (15)-(17) into (14) and according to the following formulae:

$$\begin{aligned} &\frac{\partial}{\partial z}\left[H_n^{(1)}(K|z|)\left(\frac{z}{|z|}\right)^n\right] = \frac{K}{2}H_{n-1}^{(1)}(K|z|)\left(\frac{z}{|z|}\right)^{n-1} \\ &\frac{\partial}{\partial \overline{z}}\left[H_n^{(1)}(K|z|)\left(\frac{z}{|z|}\right)^n\right] \\ &\quad = -\frac{K}{2}H_{n+1}^{(1)}(K|z|)\left(\frac{z}{|z|}\right)^{n+1} \end{aligned} \tag{19}$$

we can obtain

$$\sigma_{rz}^{(Inc)} = \frac{i\mu K W_0}{2}\left(e^{i\theta} + e^{-i\theta}\right)e^{(iK/2)(z+\overline{z})} \tag{20}$$

$$\sigma_{\theta z}^{(Inc)} = -\frac{\mu K W_0}{2}\left(e^{i\theta} - e^{-i\theta}\right)e^{(iK/2)(z+\overline{z})} \tag{21}$$

$$\begin{aligned} \sigma_{rz}^{(Sca)} &= \frac{\mu K W_0}{4}\sum_{n=0}^{+\infty} A_n\left[H_{n-1}^{(1)}(K|z|) - H_{n+1}^{(1)}(K|z|)\right] \\ &\quad \cdot \left[\left(\frac{z}{|z|}\right)^n + \left(\frac{z}{|z|}\right)^{-n}\right] \end{aligned} \tag{22}$$

$$\begin{aligned} \sigma_{\theta z}^{(Sca)} &= \frac{i\mu K W_0}{4}\sum_{n=0}^{+\infty} A_n\left[H_{n-1}^{(1)}(K|z|) + H_{n+1}^{(1)}(K|z|)\right] \\ &\quad \cdot \left[\left(\frac{z}{|z|}\right)^n - \left(\frac{z}{|z|}\right)^{-n}\right] \end{aligned} \tag{23}$$

$$\begin{aligned} \sigma_{rz}^{(Ref)} &= -\frac{\mu_I K_I W_0}{4} \\ &\quad \cdot \sum_{n=0}^{+\infty} B_n\left[J_{n-1}(K_I|z|) - J_{n+1}(K_I|z|)\right] \\ &\quad \cdot \left[\left(\frac{z}{|z|}\right)^n + \left(\frac{z}{|z|}\right)^{-n}\right] \end{aligned} \tag{24}$$

$$\begin{aligned} \sigma_{\theta z}^{(Ref)} &= -\frac{i\mu_I K_I W_0}{4} \\ &\quad \cdot \sum_{n=0}^{+\infty} B_n\left[J_{n-1}(K_I|z|) + J_{n+1}(K_I|z|)\right] \\ &\quad \cdot \left[\left(\frac{z}{|z|}\right)^n - \left(\frac{z}{|z|}\right)^{-n}\right] \end{aligned} \tag{25}$$

The corresponding stresses are

$$\begin{aligned}\sigma_{rz}^{(M)} &= \sigma_{rz}^{(Inc)} + \sigma_{rz}^{(Sca)},\\ \sigma_{\theta z}^{(M)} &= \sigma_{\theta z}^{(Inc)} + \sigma_{\theta z}^{(Sca)},\\ \sigma_{rz}^{(I)} &= \sigma_{rz}^{(Ref)},\\ \sigma_{\theta z}^{(I)} &= \sigma_{\theta z}^{(Ref)}\end{aligned} \tag{26}$$

According to the continuity of displacements, on the interface ($r = a$), we have

$$W^{(M)} = W^{(I)} \tag{27}$$

On the nanoinclusion interface, the strain component $\varepsilon_{\theta z}$ can be obtained from (2):

$$\varepsilon_{\theta z} = \frac{\sigma_{\theta z}}{2\mu} \tag{28}$$

The surface stress $\sigma_{\theta z}^{s}$ can be obtained from (6)

$$\sigma_{\theta z}^{s} = 2\mu^{s}\varepsilon_{\theta z} \tag{29}$$

Substituting (28) into (29) leads to

$$\sigma_{\theta z}^{s} = \frac{\mu^{s}}{\mu}\sigma_{\theta z} \tag{30}$$

According to (5), we can obtain the boundary conditions on the interface ($r = a$):

$$\sigma_{rz}^{(M)} - \sigma_{rz}^{(I)} = -\frac{1}{a}\frac{\partial \sigma_{\theta z}^{s}}{\partial \theta} \tag{31}$$

Substituting (30) into (31), we have the following boundary condition:

$$\sigma_{rz}^{(M)} - \sigma_{rz}^{(I)} = -s\frac{\partial \sigma_{\theta z}}{\partial \theta} \tag{32}$$

in which $s = \mu^{s}/\mu a$, which is a dimensionless parameter that reflects the interface effect at the nanoscale. For a macroscope, $s \ll 1$, and thus we can ignore the interface effect. However, when the radius of the inclusion is reduced to the nanoscale, s becomes appreciable and the interface effect should be taken into consideration [17, 21, 22].

Substituting (20)-(26) into (27) and (32), we have

$$\begin{aligned}&e^{iKa\cos\theta} + \frac{1}{2}\sum_{n=0}^{+\infty} A_n H_n^{(1)}(Ka)\left(e^{in\theta} + e^{-in\theta}\right) = -\frac{1}{2}\\ &\cdot \sum_{n=0}^{+\infty} B_n J_n(K_I a)\left(e^{in\theta} + e^{-in\theta}\right)\end{aligned} \tag{33}$$

$$\begin{aligned}&2iK\mu(1-s)\left(e^{i\theta} + e^{-i\theta}\right)e^{iKa\cos\theta} + K^2\mu as\left(e^{2i\theta} + e^{-2i\theta}\right.\\ &\left. - 2\right)e^{iKa\cos\theta} = K\mu\sum_{n=0}^{+\infty} A_n\left[(ns-1)H_{n-1}^{(1)}(Ka)\right.\\ &\left. + (ns+1)H_{n+1}^{(1)}(Ka)\right]\left(e^{in\theta} + e^{-in\theta}\right)\\ &- K_I\mu_I\sum_{n=0}^{+\infty} B_n\left[J_{n-1}(K_I a) - J_{n+1}(K_I a)\right]\left(e^{in\theta}\right.\\ &\left. + e^{-in\theta}\right)\end{aligned} \tag{34}$$

Both sides of (33) and (34) are multiplied by $e^{-im\theta}$ at the same time, then integral from 0 to 2π, and then use the following formula:

$$\int_0^{2\pi} e^{iKa\cos\theta}e^{-im\theta}d\theta = \begin{cases} 2\pi J_0(Ka) & m = 0\\ 2\pi i^{m}J_m(Ka) & m > 0\\ 2\pi i^{-m}J_{-m}(Ka) & m < 0\end{cases} \tag{35}$$

thus, the coefficients A_n, B_n can be determined as

$$\begin{aligned}A_n &= -\varepsilon_n i^{n}\frac{\mu K J_n(K_I a)M_1 + \mu_I K_I J_n(Ka)M_3}{\mu K J_n(K_I a)M_2 + \mu_I K_I H_n^{(1)}(Ka)M_3},\\ &\qquad (n = 0, 1, 2, \cdots)\\ B_n &= -\varepsilon_n i^{n}\frac{J_n(Ka) + A_n H_n^{(1)}(Ka)}{J_n(K_I a)},\\ &\qquad (n = 0, 1, 2, \cdots)\end{aligned} \tag{36}$$

in which

$$\begin{aligned}M_1 &= (ns-1)J_{n-1}(Ka) + (ns+1)J_{n+1}(Ka)\\ M_2 &= (ns-1)H_{n-1}^{(1)}(Ka) + (ns+1)H_{n+1}^{(1)}(Ka)\\ M_3 &= J_{n-1}(K_I a) - J_{n+1}(K_I a)\\ \varepsilon_n &= \begin{cases}1, & n = 0\\ 2, & n \geq 1.\end{cases}\end{aligned} \tag{37}$$

When the interface effect is neglected ($s = 0$), our results for A_n, B_n are consistent with Pao and Mow's [1] results. Thus, it can be determined that our results are correct, and the elastic scattering fields the SH-wave induces can be obtained.

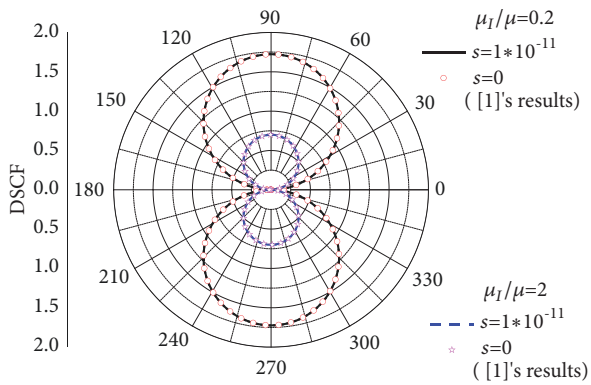

Figure 2: Comparison of the present and [1]'s results for the DSCF.

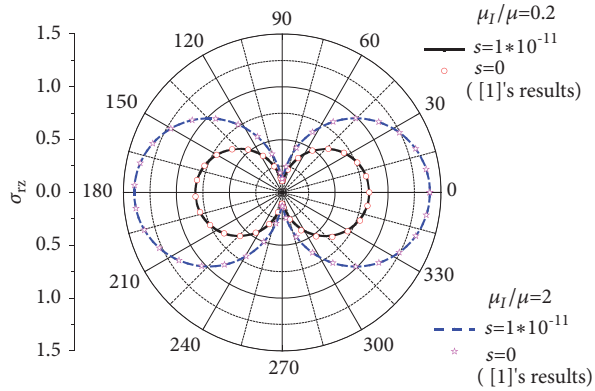

Figure 3: Comparison of the present and [1]'s results for the radial stress.

4. Numerical Results and Discussions

It is important to investigate the nanoinclusion's effects on the elastic wave-induced dynamic stress concentration, particularly at the nanoscale. Herein, the SH-wave-induced DSCF is calculated as

$$\mathrm{DSCF} = \left| \frac{\sigma_{\theta z}}{\sigma_0} \right| \tag{38}$$

in which $\sigma_{\theta z}$ is the bulk stress in the medium along the interface, and $\sigma_0 = \mu K W_0$ is the stress intensity in the SH-waves' propagation direction. From the expressions of A_n and B_n, it can be seen that when the interface effect is taken into account, the DSCF and radical stress depend not only on the wave number but also on the interface elasticity parameter.

In what follows, we investigate the influence of the interface effect and nanoinclusion on the DSCF and the radial stress.

To verify the formulation of the present paper, we compare our numerical results with those of Pao's, as shown in Figures 2 and 3. It can be seen that these results for the DSCF and the radial stress around a circular nanoinclusion are consistent with the Pao's results [1]. On the other hand, we can see that as the circular inclusion's hardness increases, the DSCF decreases and the radial stress increases.

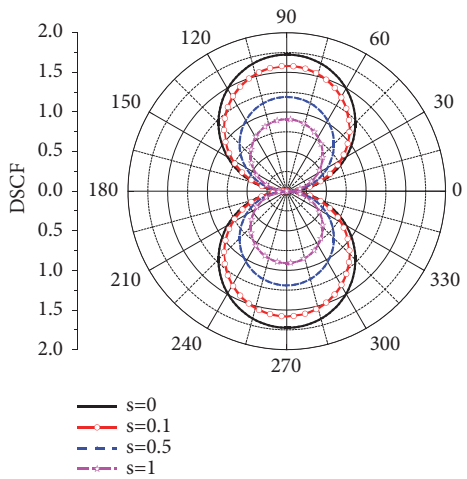

Figure 4: Effect of interface effect on the DSCF with $K_I/K = 0.2$.

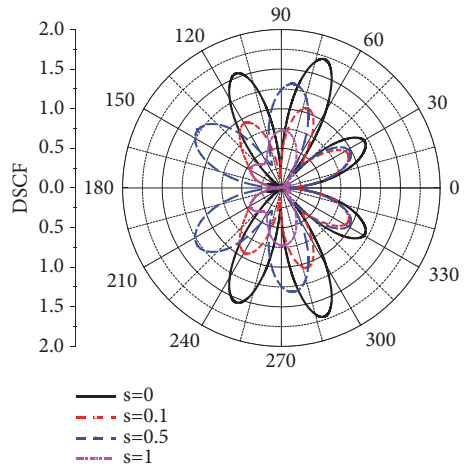

Figure 5: Effect of interface effect on the DSCF with $K_I/K = \pi$.

For a softer nanoinclusion i.e., $\mu_I/\mu = 0.2$, the DSCF's distributions on the interface for different values of s with $K_I/K = 0.2$ are shown in Figure 4, which indicates clearly the interface's significant effect on the dynamic stress concentration near the inclusion. As s increases, the DSCF decreases continuously. Similarly, the DSCF's distributions on the interface for different values of s with $K_I/K = \pi$ are shown in Figure 5, which also demonstrates clearly the interface's significant effect on the dynamic stress concentration near the nanoinclusion. Again, as s increases, the DSCF decreases in most regions.

To examine the effect of soft and hard nanoinclusions, the DSCF near the nanoinclusion for various ratios of shear modulus μ_I/μ with $K_I/K = 0.2$ and $s = 0.5$ are shown in Figure 6. For a soft inclusion ($\mu_I/\mu < 1$), the stress concentration is much larger than that for a hard inclusion ($\mu_I/\mu > 1$). Similarly, The DSCF near the nanoinclusion for various ratios of shear modulus μ_I/μ with $K_I/K = \pi$ and $s = 0.5$ are shown in Figure 7, and the results are the same as those for $K_I/K = 0.2$.

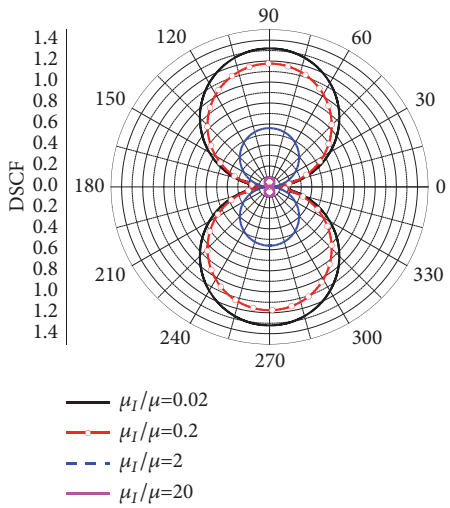

Figure 6: Effect of μ_I/μ on the DSCF with $K_I/K = 0.2$.

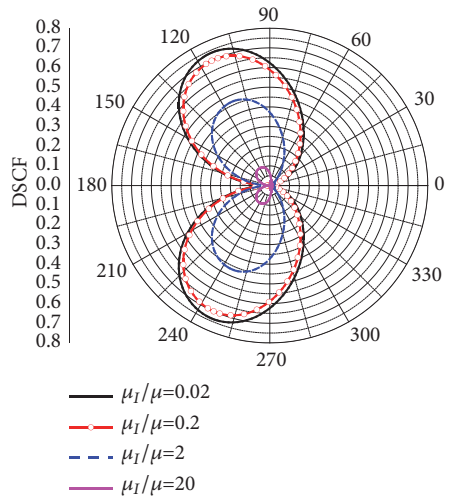

Figure 7: Effect of μ_I/μ on the DSCF with $K_I/K = \pi$.

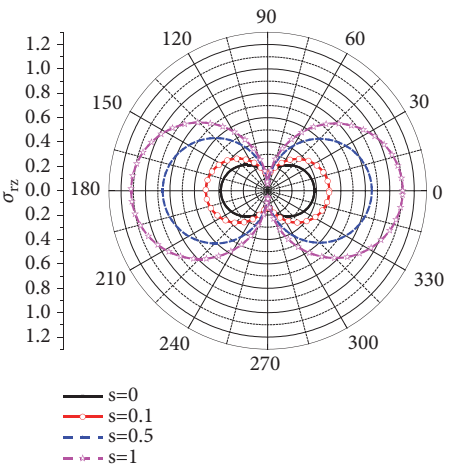

Figure 8: Effect of interface effect on the radial stress with $K_I/K = 0.2$.

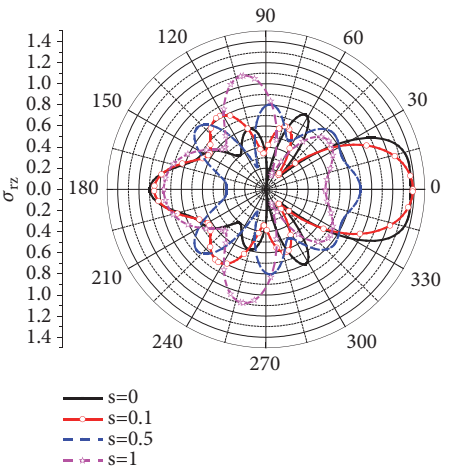

Figure 9: Effect of interface effect on the radial stress with $K_I/K = \pi$.

For a softer nanoinclusion, i.e., $\mu_I/\mu = 0.2$, the radial stress' distributions on the interface for different values of s with $K_I/K = 0.2$ are shown in Figure 8, which indicates clearly the interface's significant effect on the radial stress near the inclusion. As s increases, the radial stress increases continuously. Similarly, the DSCF's distributions on the interface for different values of s with $K_I/K = \pi$ are shown in Figure 9 and demonstrate clearly the interface's significant effect on the radial stress near the inclusion. As s increases, the radial stress increases in most regions. However, when $\theta = 0$, the radial stress decreases as s increases.

The radial stress near the nanoinclusion for various ratios of shear modulus μ_I/μ with $K_I/K = 0.2$ and $s = 0.5$ are shown in Figure 10. For a soft nanoinclusion ($\mu_I/\mu < 1$), the radial stress is much smaller than that for a hard nanoinclusion ($\mu_I/\mu > 1$). Similarly, the radial stress near the nanoinclusion for various ratios of shear modulus μ_I/μ with $K_I/K = \pi$ and $s = 0.5$ are shown in Figure 11, and the results are the same as those for $K_I/K = 0.2$ in most regions. The figures show

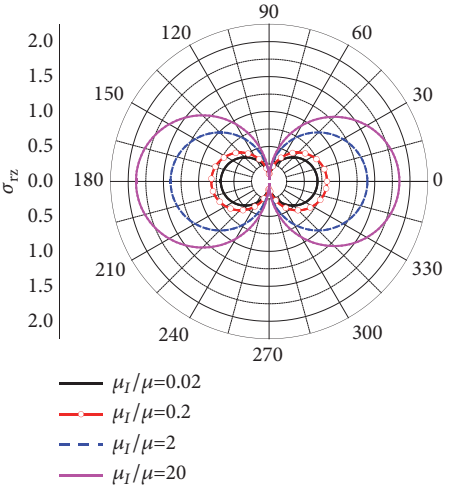

Figure 10: Effect of μ_I/μ on the radial stress with $K_I/K = 0.2$.

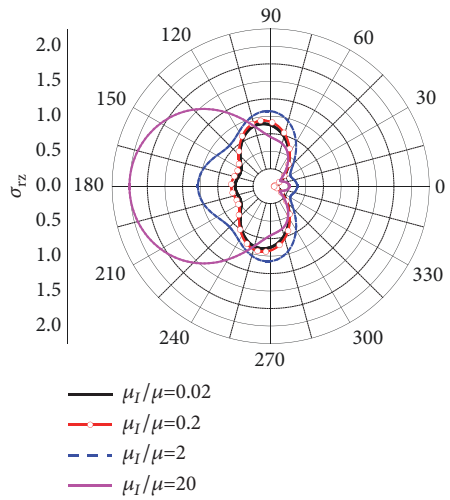

FIGURE 11: Effect of μ_I/μ on the radial stress with $K_I/K = \pi$.

that the distribution of the radial stress differs from that of the DSCF.

The numerical results show that the interface effect has a significant influence on the stress concentration and the radial stress. At the same time, they clearly are affected differentially by soft and hard nanoinclusions.

5. Conclusion

In this paper, the method of complex variable function is used to study SH-waves' scattering by a circular nanoinclusion. Based on the classical elasticity and the surface elasticity theories, the analytical solution of the stress field is obtained by the orthogonality of trigonometric functions. Finally, the influence of the interface effect s and the ratios of shear modulus μ_I/μ on the DSCF and the radial stress around the nanoinclusion are analyzed to obtain numerical results. From these results, we can see that the conclusion obtained by using the complex function method is similar to what previous scholars have obtained by other methods. Therefore, our research method has clear theoretical value. The results show that (1) the interface effect weakens the dynamic stress concentration around the nanoinclusion, and when the radius is sufficiently large, the interface effect can be neglected; (2) the interface effect enhances the radial stress's effect. When the other variables are fixed, the radials stress gets larger as the inclusion radius decreases; (3) as the shear modulus ratios increases, the DSCF decreases, while the radial stress increases.

Data Availability

No data were used to support this study.

Conflicts of Interest

The author declares that they have no conflicts of interest.

Acknowledgments

The author Hongmei Wu was supported by National Natural Science Foundation of China (11862014).

References

[1] Y. Pao H and C. Mow C, *Diffraction of Elastic Waves and Dynamic Stress Concentrations*, Crane Russak, New York, NY, USA, 1973.

[2] L. Diankui, "Dynamic stress concentration around a circular hole due to SH-wave in anisotropic media," *Acta Mechanica Sinica*, vol. 4, no. 2, pp. 146–155, 1988.

[3] D. Liu and J. Tian, "Scattering and dynamic stress concentration of sh-wave by interface cylindrical elastic inclusion," *Expolosion and Shock Waves*, vol. 19, no. 2, pp. 115–123, 1999.

[4] B. Hei, Z. Yang, B. Sun, and Y. Wang, "Modelling and analysis of the dynamic behavior of inhomogeneous continuum containing a circular inclusion," *Applied Mathematical Modelling: Simulation and Computation for Engineering and Environmental Systems*, vol. 39, no. 23-24, pp. 7364–7374, 2015.

[5] D. R. McArthur and L. J. Sudak, "A circular inclusion with circumferentially inhomogeneous imperfect interface in harmonic materials," *Continuum Mechanics and Thermodynamics*, vol. 28, no. 1-2, pp. 317–329, 2016.

[6] G. Jiang, Z. Yang, C. Sun, B. Sun, and Y. Yang, "Dynamic response of a circular inclusion embedded in inhomogeneous half-space," *Archive of Applied Mechanics*, vol. 88, no. 10, pp. 1791–1803, 2018.

[7] E. W. Wong, P. E. Sheehan, and C. M. Lieber, "Nanobeam mechanics: elasticity, strength, and toughness of nanorods and nanotubes," *Science*, vol. 277, no. 5334, pp. 1971–1975, 1997.

[8] M. E. Gurtin, J. Weissmüller, and F. Larché, "A general theory of curved deformable interfaces in solids at equilibrium," *Philosophical Magazine*, vol. 78, no. 5, pp. 1093–1109, 1998.

[9] R. E. Miller and V. B. Shenoy, "Size-dependent elastic properties of nanosized structural elements," *Nanotechnology*, vol. 11, no. 3, pp. 139–147, 2000.

[10] V. B. Shenoy, "Size-dependent rigidities of nanosized torsional elements," *International Journal of Solids and Structures*, vol. 39, no. 15, pp. 4039–4052, 2002.

[11] P. Sharma, S. Ganti, and N. Bhate, "Effect of surfaces on the size-dependent elastic state of nano-inhomogeneities," *Applied Physics Letters*, vol. 82, no. 4, pp. 535–537, 2003.

[12] F. Yang, "Size-dependent effective modulus of elastic composite materials: Spherical nanocavities at dilute concentrations," *Journal of Applied Physics*, vol. 95, no. 7, pp. 3516–3520, 2004.

[13] G. F. Wang, T. J. Wang, and X. Q. Feng, "Surface effects on the diffraction of plane compressional waves by a nanosized circular hole," *Applied Physics Letters*, vol. 89, no. 23, Article ID 231923-3, 2006.

[14] G. F. Wang, "Diffraction of plane compressional wave by a nanosized spherical cavity with surface effects," *Applied Physics Letters*, vol. 90, no. 21, p. 211907-3, 2007.

[15] G. F. Wang, "Multiple diffraction of plane compressional waves by two circular cylindrical holes with surface effects," *Journal of Applied Physics*, vol. 105, no. 1, p. 013507-6, 2009.

[16] Z. Y. Ou and D. W. Lee, "Effects of interface energy on scattering of plane elastic wave by a nano-sized coated fiber," *Journal of Sound and Vibration*, vol. 331, no. 25, pp. 5623–5643, 2012.

[17] Y. Ru, G. F. Wang, and T. J. Wang, "Diffractions of elastic waves and stress concentration near a cylindrical nano-inclusion incorporating surface effect," *Journal of Vibration and Acoustics*, vol. 131, no. 6, pp. 1747–1750, 2009.

[18] Y. Ru, G. F. Wang, L. C. Su, and T. J. Wang, "Scattering of vertical shear waves by a cluster of nanosized cylindrical holes with surface effect," *Acta Mechanica*, vol. 224, no. 5, pp. 935–944, 2013.

[19] R. Yan, "Surface effect on diffractions of elastic waves and stress concentration near a cluster of cylindrical nanoholes arranged as quadrate shape," *Advances in Materials Science and Engineering*, vol. 2015, Article ID 134975, 8 pages, 2015.

[20] H. M. Wu and Z. Y. Ou, "Scattering of SH-wave by a cylindrical of nano-inclusion with interface effect," in *Proceedings of the 2014 International Conference on Energy, Environment and Materials Engineering*, pp. 918–922, Guangdong, China, February 2014.

[21] L. H. He and Z. R. Li, "Impact of surface stress on stress concentration," *International Journal of Solids and Structures*, vol. 43, no. 20, pp. 6208–6219, 2006.

[22] L. Tian and R. K. N. D. Rajapakse, "Elastic field of an isotropic matrix with a nanoscale elliptical inhomogeneity," *International Journal of Solids and Structures*, vol. 44, no. 24, pp. 7988–8005, 2007.